Numerical Simulation of the Aerodynamics and Acoustics of a Turbulent Wall Jet with Particulates

Wei Wang, Trushant Patel,

S. Balachandar, and S. A. E. Miller

University of Florida
Theoretical Fluid Dynamics and Turbulence Group

Acknowledgement

Dr. Thomas Jackson

Rahul Koneru

This research is supported by the University of Florida Department of Mechanical and Aerospace Engineering and the Herbert Wertheim College of Engineering.

Outline

- Introduction and Background
- Computational Approach
- Results
  - Flow
  - Aeroacoustics
- Summary and Conclusion

Introduction and Background

Rocket Exhaust Noise

Objective: Understanding the physics of noise generation and propagation of two-phase particle-gas supersonic jet flow, and build the tool to make prediction.

Counter, D. and Houston, J., "Ares I Scale Model Acoustic Test Above Deck Water Sound Suppression Results," 162nd Acoustical Society of America Meeting, 2011.

Previous Investigations (Select)

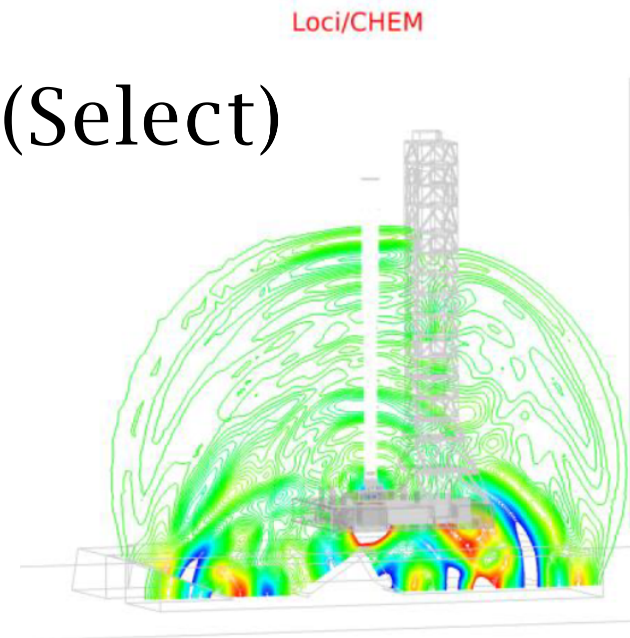

- NASA Marshall
  - Ares I Scale Model Acoustic Test (ASMAT)
  - Loci/CHEM code
- NASA AMES
  - Launch, Ascent, and Vehicle Aerodynamics (LAVA) code

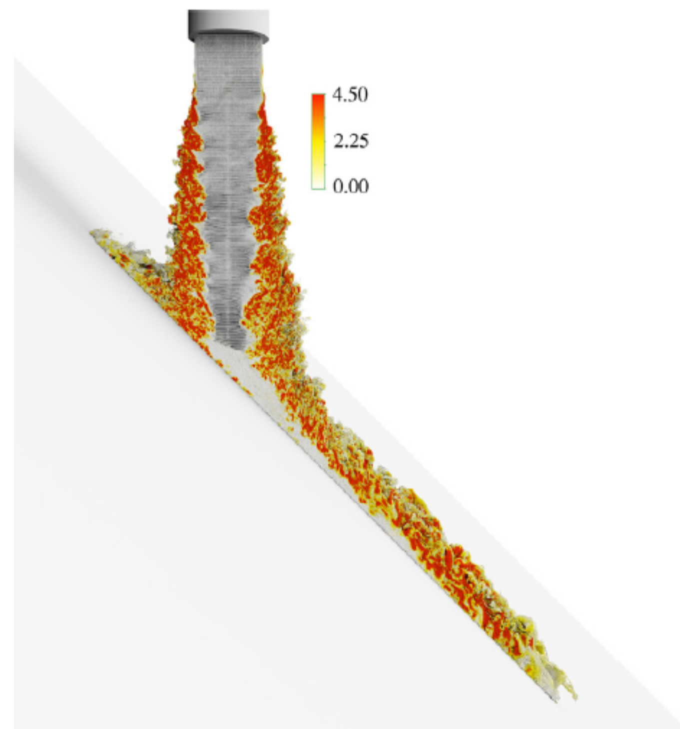

Counter, D. and Houston, J., "Ares I Scale Model Acoustic Test Above Deck Water Sound Suppression Results," 162nd Acoustical Society of America Meeting, 2011.

Kiris, C. C., Housman, J. A., Barad, M. F., Brehm, C., Sozer, E., and Moini-Yekta, S., "Computational framework for Launch, Ascent, and Vehicle Aerodynamics (LAVA)," *Aerospace Science and Technology*, vol. 55, 2016, pp. 189–219.

Computational Approach

Numerical Simulation

- RocfluMP CFD Solver
- Unstructured
- Finite Volume
- Eulerian-Lagrangian
- 2-Way Coupling
- Implicit LES
- AUSM+
- 3rd order Runge-Kutta

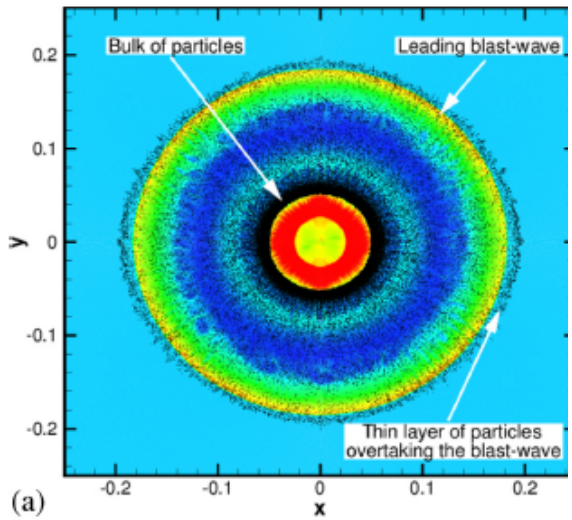

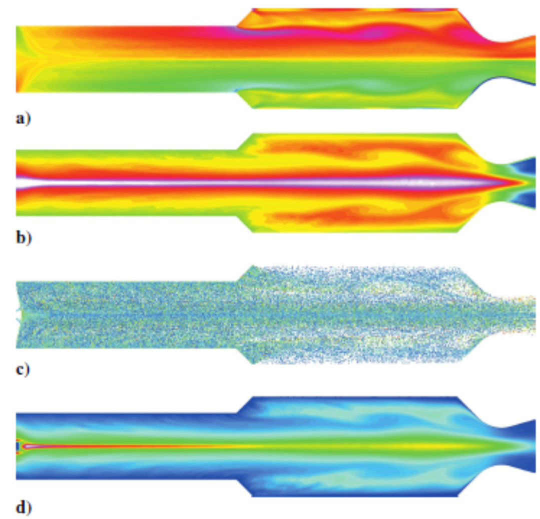

Najjar, F., Ferry, J., Haselbacher, A., and Balachandar, S., "Simulations of solid-propellant rockets: effects of aluminum droplet size distribution," Journal of Spacecraft and Rockets, Vol. 43, No. 6, 2006, pp. 1258.

Annamalai, S., Rollin, B., Ouellet, F., Neal, C., Jackson, T. L., and Balachandar, S., "Effects of initial perturbations in the early moments of an explosive dispersal of particles," Journal of Fluids Engineering, Vol. 138, No. 7, 2016, pp. 070903.

Governing Equation of Gas

Navier-Stokes Equation

$$\frac{\partial}{\partial t}\int_{\Omega} \boldsymbol{W} d\Omega + \oint_{\partial\Omega} \boldsymbol{F_c} dS = \oint_{\partial\Omega} \boldsymbol{F_v} dS + \int_{\Omega} \boldsymbol{Q} d\Omega$$

where

$$\boldsymbol{W} = [\rho, \rho u, \rho v, \rho w, \rho E]^T$$

$$\boldsymbol{F_c} = \left[\rho V_n, \rho u V_n + n_x p, \rho v V_n + n_y p, \rho w V_n + n_z p, \rho H V_n\right]^T$$

$$\boldsymbol{F_v} = \begin{bmatrix} 0 \\ n_x\tau_{xx} + n_y\tau_{xy} + n_z\tau_{xz} \\ n_x\tau_{yx} + n_y\tau_{yy} + n_z\tau_{yz} \\ n_x\tau_{zx} + n_y\tau_{zy} + n_z\tau_{zz} \\ n_x\Theta_x + n_y\Theta_y + n_z\Theta_z \end{bmatrix}, \begin{matrix} \Theta_x = u\tau_{xx} + v\tau_{xy} + w\tau_{xz} + k\partial T/\partial x \\ \Theta_y = u\tau_{yx} + v\tau_{yy} + w\tau_{yz} + k\partial T/\partial y \\ \Theta_x = u\tau_{zx} + v\tau_{zy} + w\tau_{zz} + k\partial T/\partial z \end{matrix}$$

Governing Equation of Gas

$$\frac{\partial}{\partial t}\int_{\Omega} \boldsymbol{W}\, d\Omega + \oint_{\partial\Omega} \boldsymbol{F}_{\boldsymbol{c}}\, dS = \oint_{\partial\Omega} \boldsymbol{F}_{\boldsymbol{v}}\, dS + \int_{\Omega} \boldsymbol{Q}\, d\Omega$$

Source terms

$$\boldsymbol{Q} = \left[0, f_{p,x}, f_{p,y}, f_{p,z}, E_p\right]^T$$

$$\boldsymbol{f}_{\boldsymbol{p}} = -\sum \frac{m_p\left(\boldsymbol{V} - \boldsymbol{V}_{\boldsymbol{p}}\right)}{\tau^u}$$

$$E_p = \sum \left[\boldsymbol{f}_{\boldsymbol{p}} \cdot \left(\boldsymbol{V}_{\boldsymbol{p}} - \boldsymbol{V}\right) - \frac{m_p C_{p,p}\left(T - T_p\right)}{\tau^\theta}\right]$$

Governing Equation of Particles

Point Particles

- Evolution Equations

$$\frac{d}{dt}\boldsymbol{x}_p = \boldsymbol{V}_p\ ,\ \frac{\mathrm{d}}{\mathrm{dt}}\mathbf{V}_\mathrm{p} = \frac{\mathbf{V}-\mathbf{V}_\mathrm{p}}{\tau^u},\ \frac{d}{d_t}T_p = \frac{T-T_p}{\tau^\theta}$$

- Time Scales

$$\tau^u = \frac{\rho_p d_p^2}{18\mu f_u(Re)},\ \tau^\theta = \frac{C_{p,p}\rho_p d_p^2}{12k f_\theta(Re)}$$

- Correlations

Naumann and Schiller(1935): $f_u(Re) = 1 + 0.15Re^{0.687}$

Ranz and Marshall(1952): $f_\theta(Re) = 1 + 0.3Re^{\frac{1}{2}}Pr^{\frac{1}{3}}$

Ffowcs-William Hawking Equation

Inhomogeneous Wave Equation Derived from Navier-Stokes Equation

$$\square^2[p'H(f)] = \frac{\partial}{\partial t}[\rho_0 v_n \delta(f)] + \frac{\partial}{\partial t}[\rho(u_n - v_n)\delta(f)]$$

$$- \frac{\partial}{\partial x_i}[\rho u_i(u_n - v_n)\delta(f)] + \frac{\partial}{\partial x_i}[L_i \delta(f)]$$

$$+ \frac{\partial^2}{\partial x_i \partial x_j}[T_{ij} H(f)]$$

Thickness noise

Loading noise

Quadrupole source

Wave operator $\square^2 = \frac{1}{c^2}\frac{\partial^2}{\partial t^2} - \frac{\partial^2}{\partial x_i^2}$

$$L_i = -\left[(p - p_0)\delta_{ij} - \sigma_{ij}\right]\widehat{n_j}$$

$$T_{ij} = \rho u_i u_j - \sigma_{ij} + [(p - p_0) - c_0^2 \rho']\delta_{ij}$$

Ffowcs-William Hawking Equation

Farrasat’s Formulation

$4\pi p'(\boldsymbol{x},t)$

$$= \int \Bigg[\frac{\rho_0 \dot{v_n}}{r(1-M_r)^2} + \frac{\rho_0 v_n \left(r\dot{M}_r + c(M_r - M^2) \right)}{r^2(1-M_r)^3} + \frac{\dot{l_r}}{cr(1-M_r)^2} + \frac{l_r - l_i \cdot M_i}{r(1-M_r)^2}$$

$$+ \frac{l_r \left(r\dot{M}_r + c(M_r - M^2) \right)}{cr^2(1-M_r)^3} + \left(\frac{\dot{\rho}(u_n - v_n) + \rho(\dot{u_n} - \dot{v_n})}{r(1-M_r)^2} \right)(1+\mathcal{M}_r)$$

$$+ \frac{\rho(u_n - v_n)}{r(1-M_r)^2}\dot{\mathcal{M}}_r + \frac{\rho(u_n - v_n)(u_r - u_i M_i)}{r^2(1-M_r)^2}$$

$$+ \frac{\rho(u_n - v_n)(1+\mathcal{M}_r)}{r^2(1-M_r)^3}\left(r\dot{M}_r + c(M_r - M^2) \right) \Bigg]_{ret} dS$$

$r = |\boldsymbol{x} - \boldsymbol{y}|$

Subscripts:

n = surface normal direction

r = radiation direction

Evaluate Far-Field Acoustics

Acoustics Solver

- Ffowcs-Williams and Hawking's (FW-H) acoustics analogy
- Developed in-house
- Any type of nozzle
- Wide range of flow conditions
- Three-dimension
- Far-field acoustics

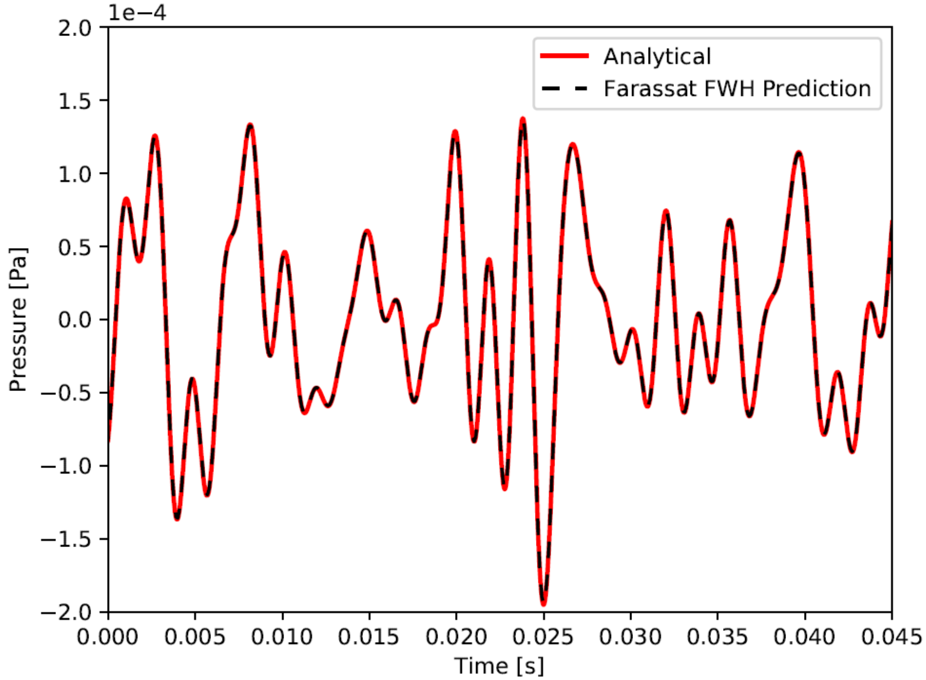

Results

Geometry

- Reproduction of experiment of Mora et al.
- Design Mach number 1.5
- Rectangular nozzle
- Aspect ratio 2
- Equivalent diameter

  $D_e = 20.65\, mm$
- Flushing-mounted plate

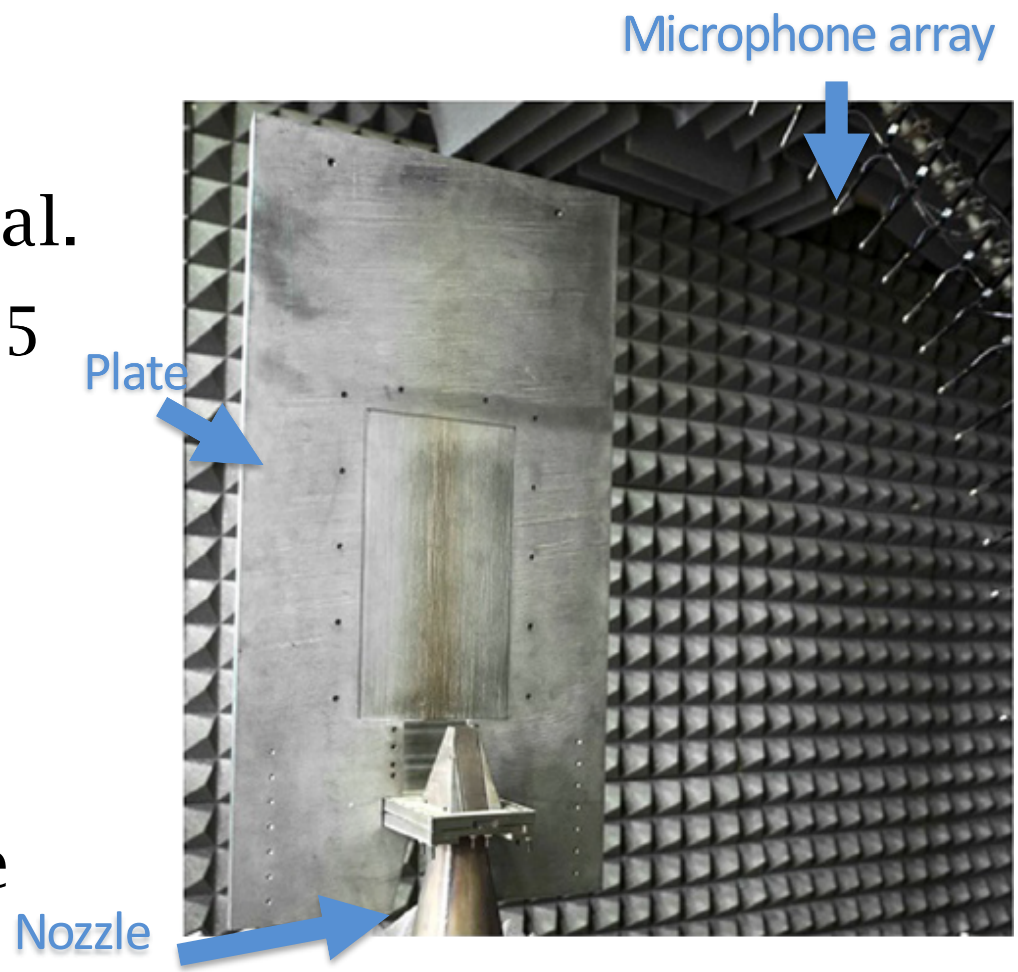

Mora, P., Baier, F., Kailasanath, K., and Gutmark, E. J., “Acoustics from a Rectangular Supersonic Nozzle Exhausting over a Flat Surface," The Journal of the Acoustical Society of America, Vol. 140, No. 6, dec 2016, pp. 4130-4141.

Geometry

2D nozzle and plate geometry, unit [mm]

X-Y plane

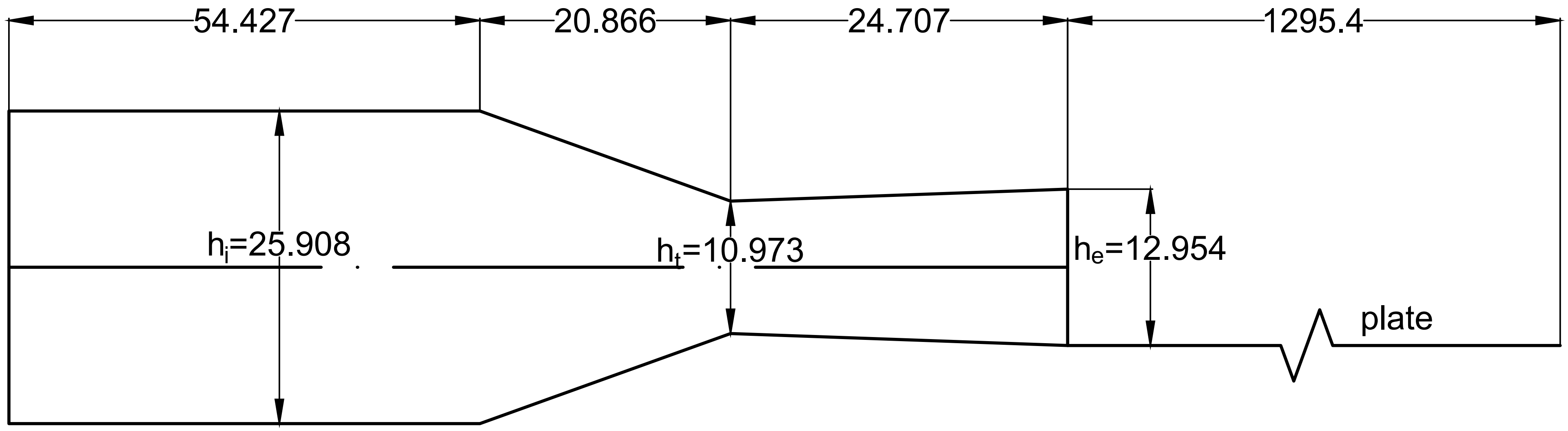

Mora, P., Baier, F., Kailasanath, K., and Gutmark, E. J., "Acoustics from a Rectangular Supersonic Nozzle Exhausting over a Flat Surface," The Journal of the Acoustical Society of America, Vol. 140, No. 6, dec 2016, pp. 4130-4141.

Grid

- 787,500 hexahedra cells
- Minimum cell $\sim 10^{-5}[m]$
- Highly clustered toward shear layer region, nozzle throat, and nozzle exit plane

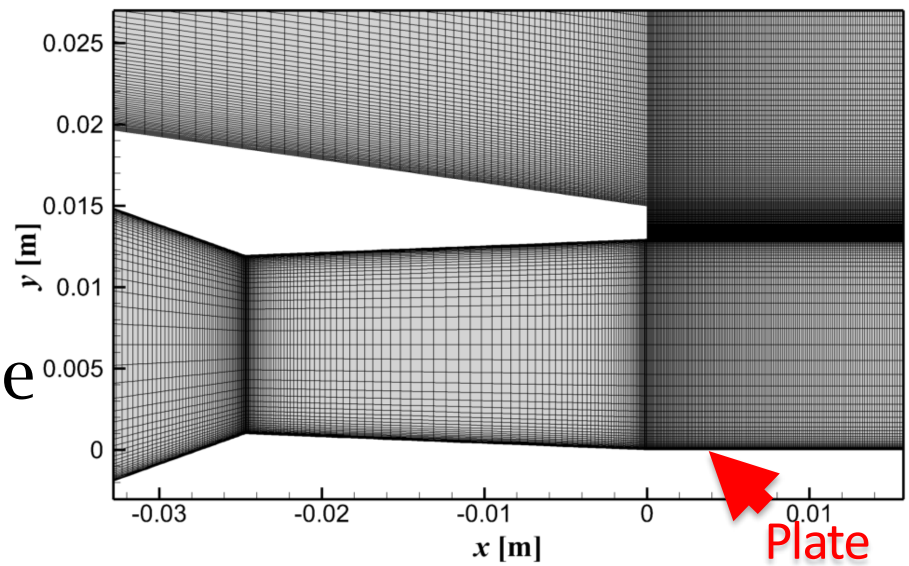

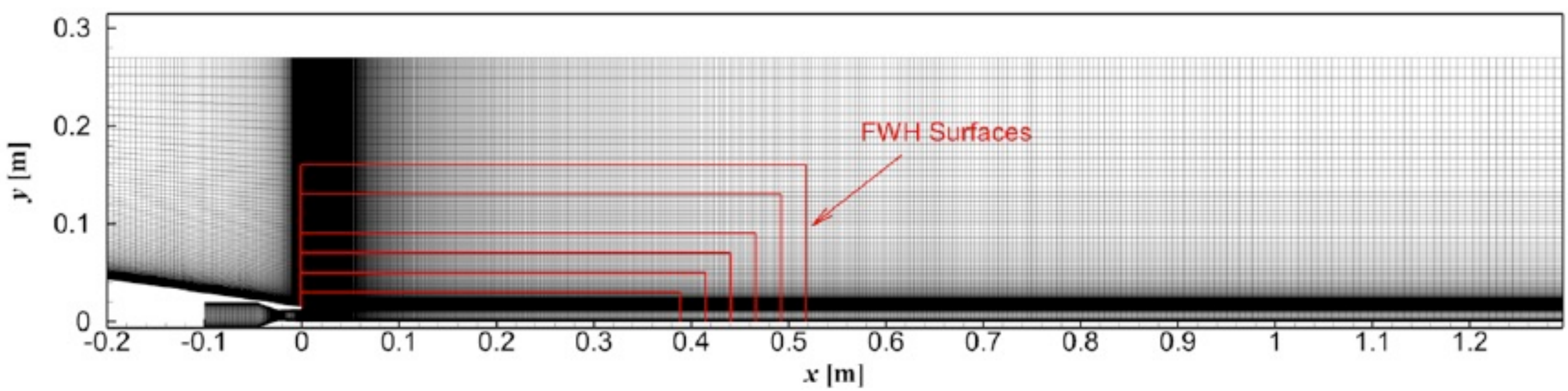

Flow-Conditions

Flow conditions for gas

Case	M_j	NPR	TTR	D_j $[mm]$	U_j [m/s]	Re_j $[\times 10^5]$
1	1.22	2.5	1.1	11.39	385.0	2.9
2	1.5	3.67	1.1	12.91	448.1	3.8
3	1.64	4.5	1.1	14.07	475.8	4.4

Particle flow conditions

Case	M_j	T_p $[K]$	ρ_p $[kg/m^3]$	Mass Loading	d_p $[\mu m]$	Super Particle Loading
1	1.5	293	1766	0.001	10	10
2	1.5	293	1766	0.001	100	1

Numerical Schlieren

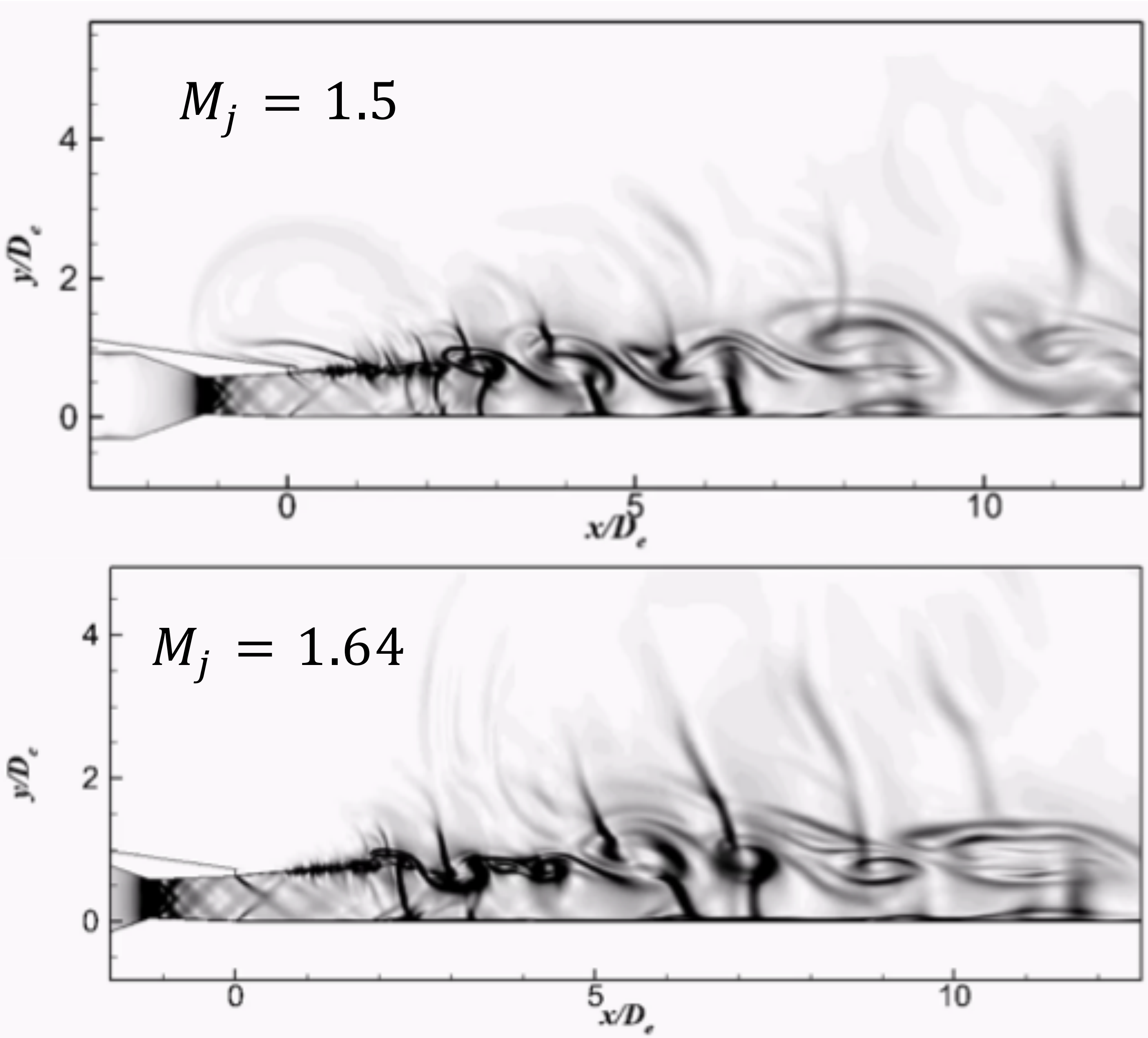

- Expansion waves in the nozzle due to the straight nozzle wall
- Mach wave propagates downstream
- Shock wave

Mean Streamwise Velocity

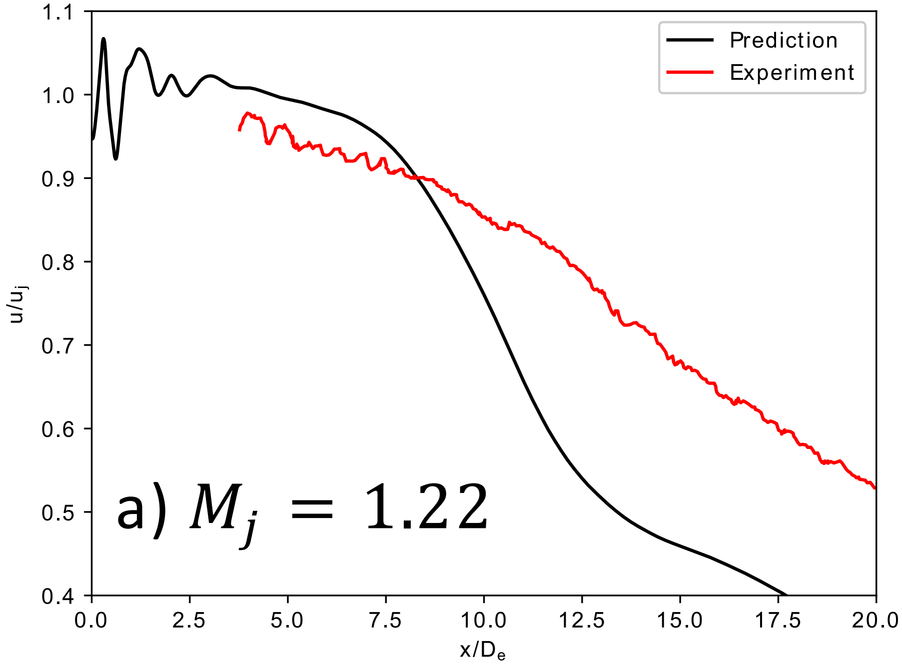

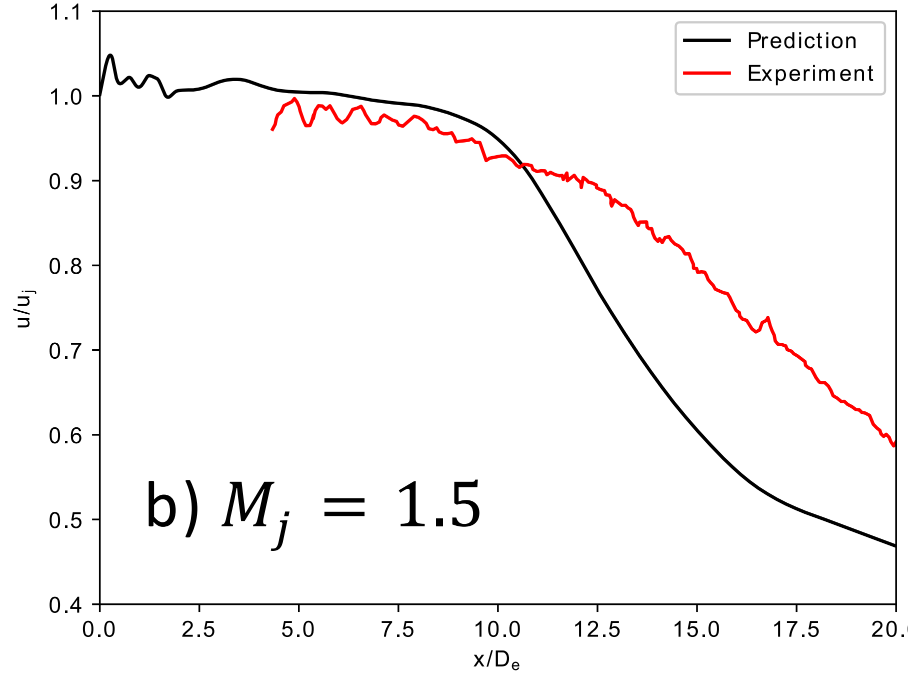

Comparison of predicted and measured time averaged streamwise velocity on the nozzle centerline.

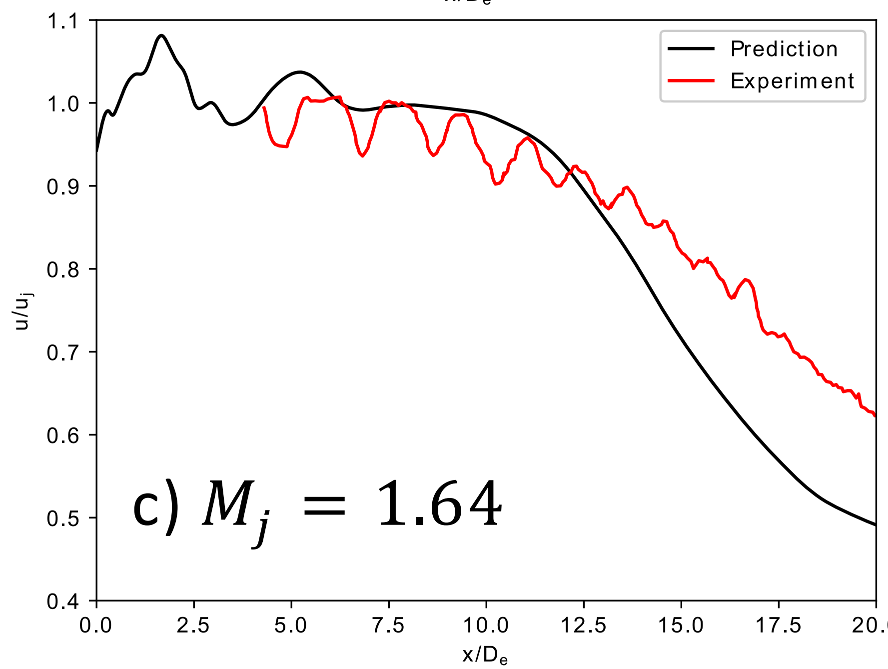

Mean Streamwise Velocity

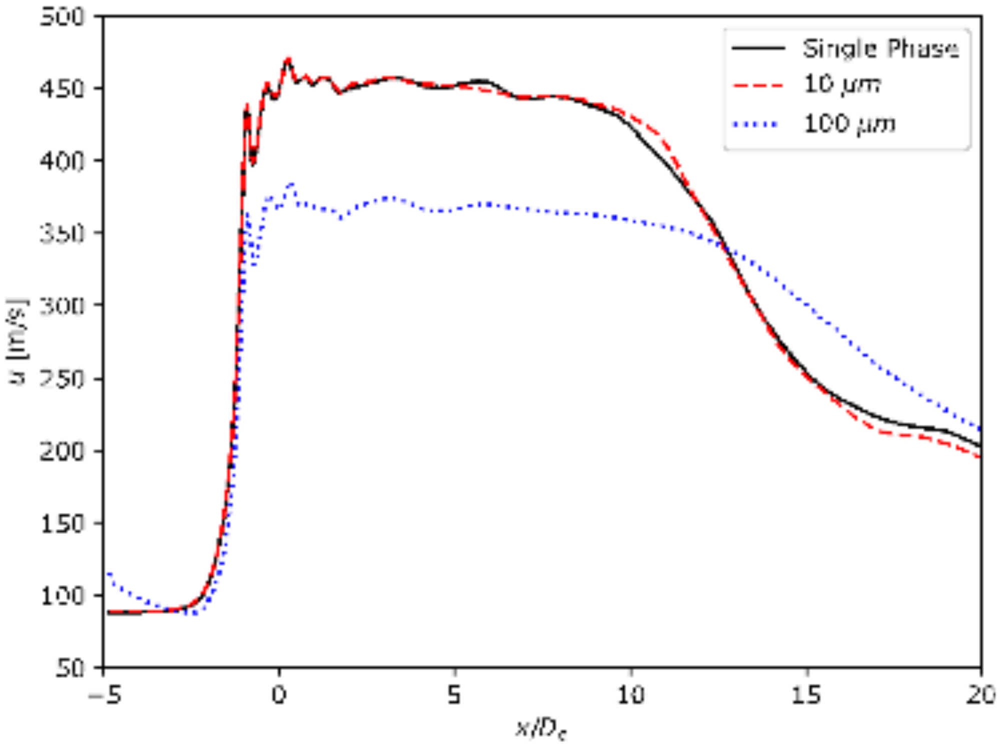

a) Mean streamwise velocity

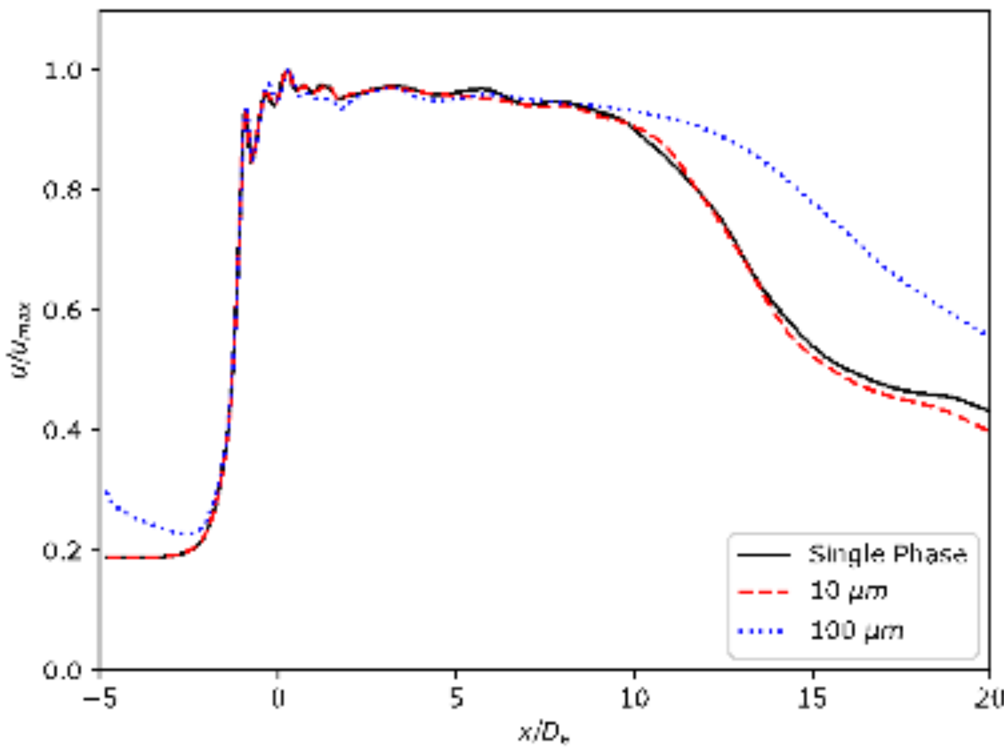

b) Normalized mean streamwise velocity

Comparison of time averaged streamwise velocity on the centerline of nozzle of single phase jet and two-phase jet with various particle diameters.

Mean Pressure

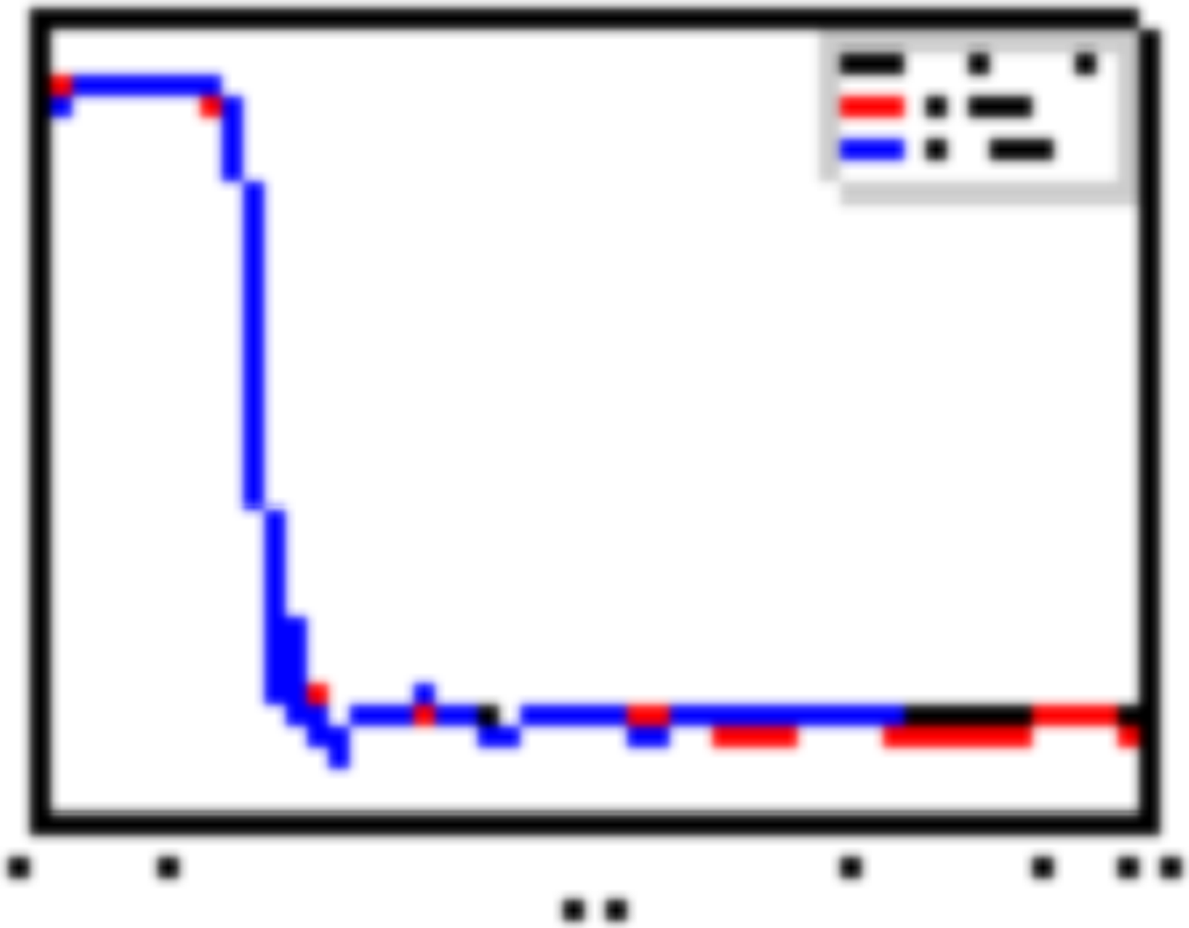

Comparison of time averaged pressure on the nozzle centerline of single phase jet and two-phase jet with various particle diameters

Turbulent Kinetic Energy

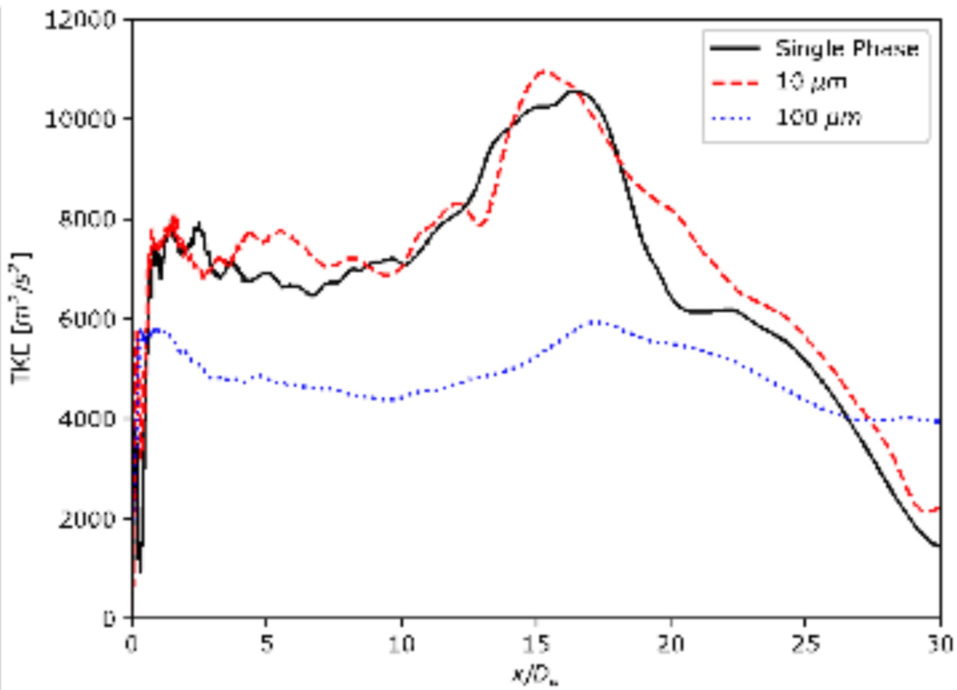

Top: Comparison of turbulent kinetic energy on the lip line with particles of diameter $10\mu m$ and $100\mu m$.

Bottom: Contour plot of turbulent kinetic energy with particles of diameter of $10\mu m$

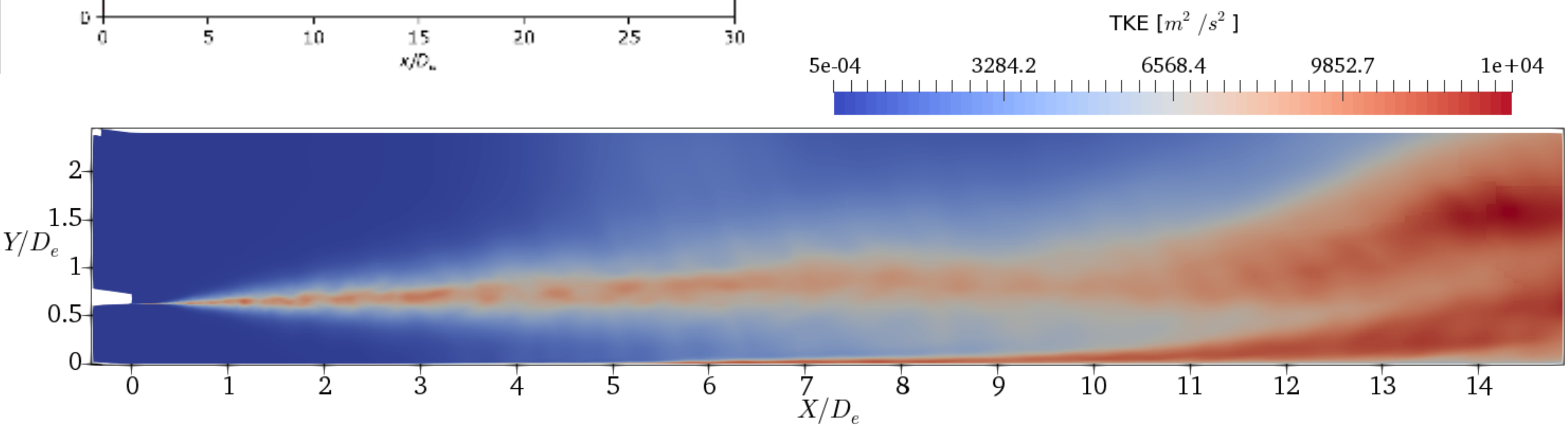

Numerical Schlieren with Particles

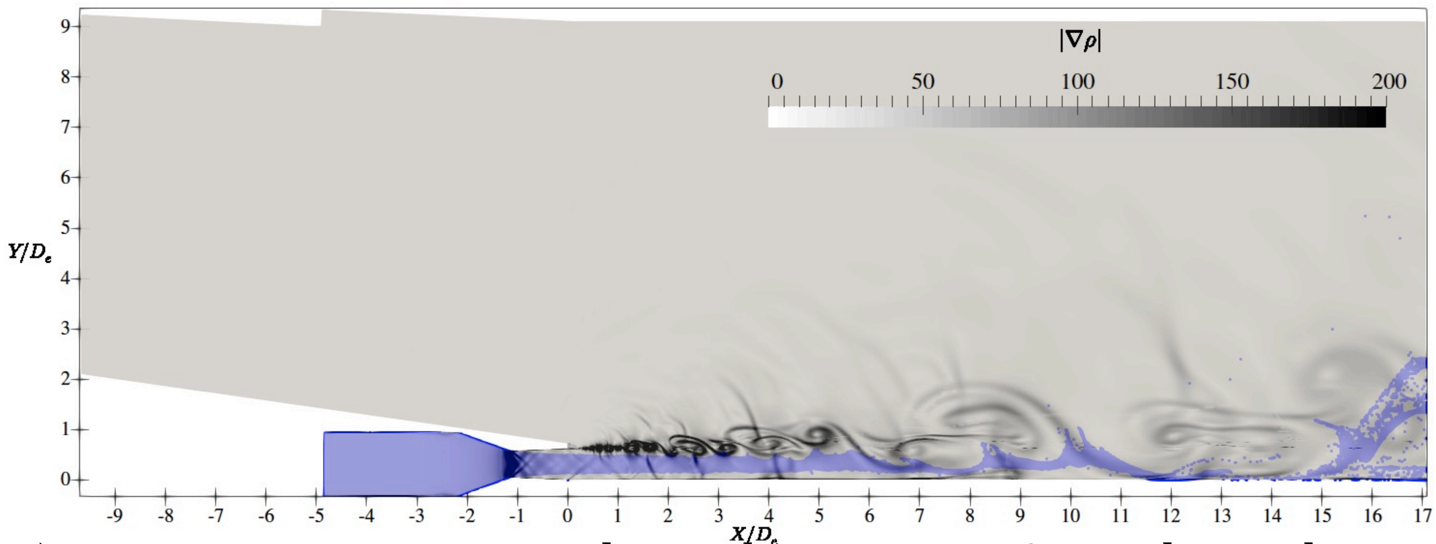

a) $d_p = 10\mu m$, 1 computational particle represent 10 actual particles.

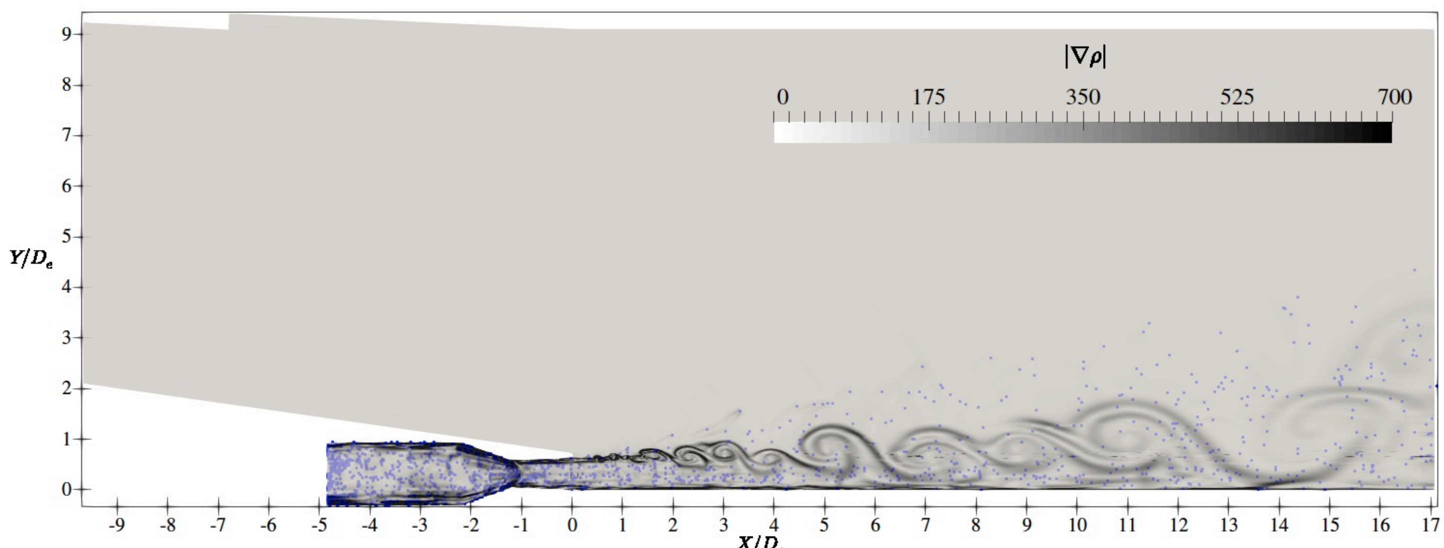

b) $d_p = 100\mu m$, 1 computational particle represent 1 actual particle.

Comparison of Instantaneous Numerical Schlieren of Flow with Various Particle Diameters.

Blue points represent computational particles in the domain.

Comparison of Predicted and Measured SPL Spectra for Various M_j

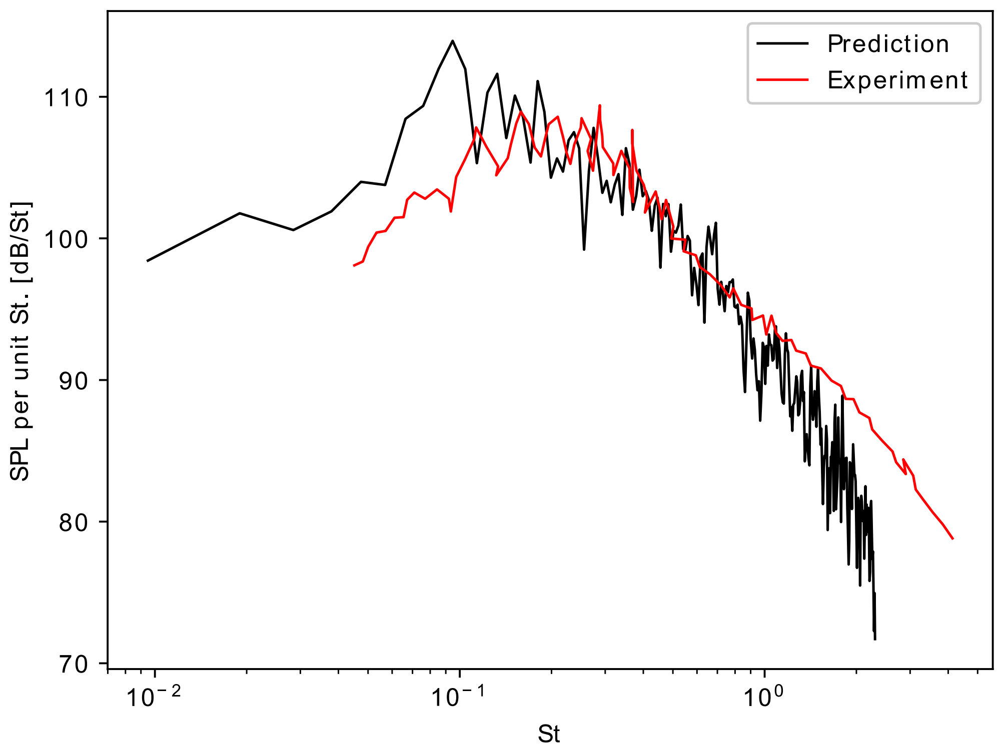

a) $M_j = 1.5, \theta = 152°$

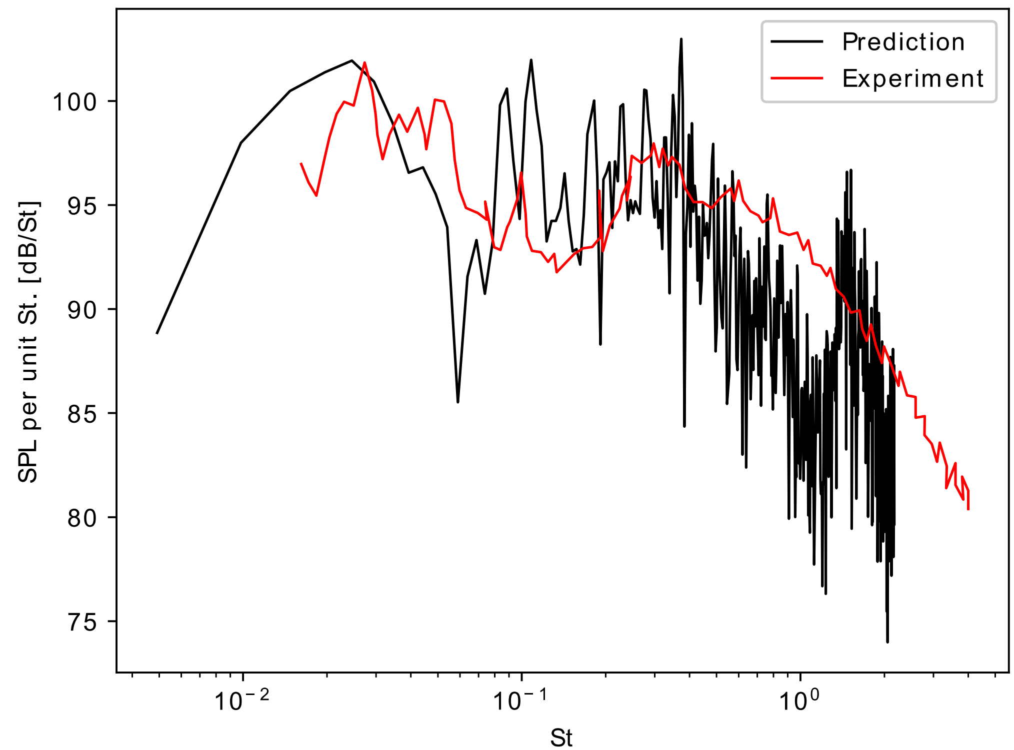

b) $M_j = 1.64, \theta = 70°$

Mora, P., Baier, F., Kailasanath, K., and Gutmark, E. J., “Acoustics from a Rectangular Supersonic Nozzle Exhausting over a Flat Surface," The Journal of the Acoustical Society of America, Vol. 140, No. 6, dec 2016, pp. 4130-4141.

Comparison of Two-Point Cross-Correlation of T_{11} of Lighthill's Stress Tensor

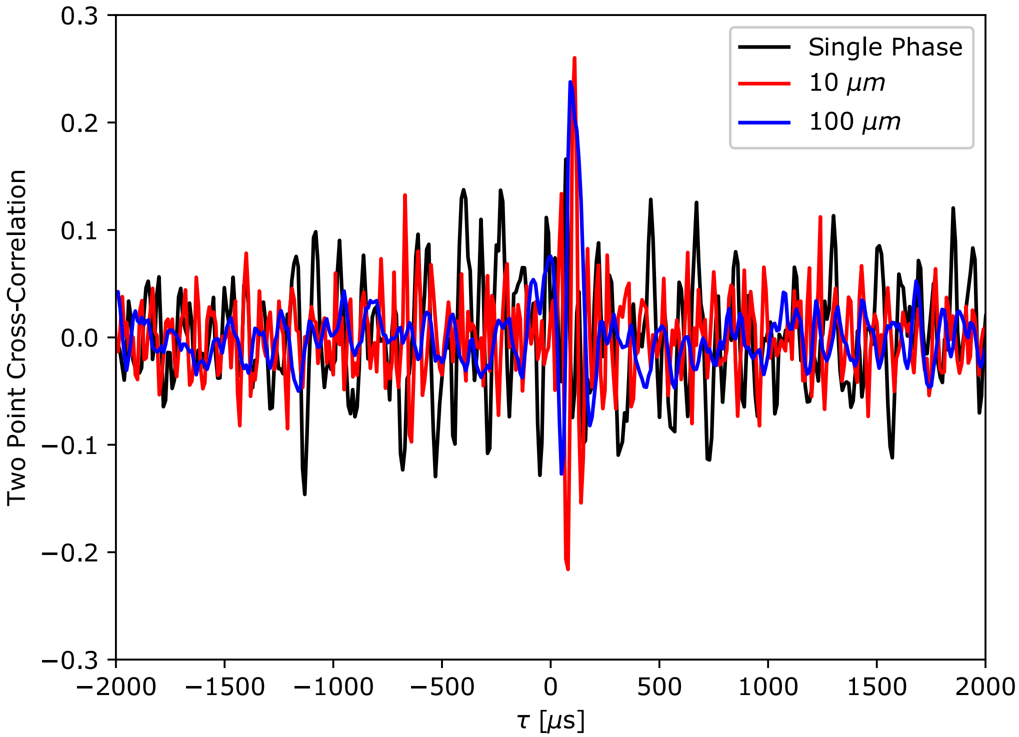

a) $-2000 \leq \tau \leq 2000 \mu s$

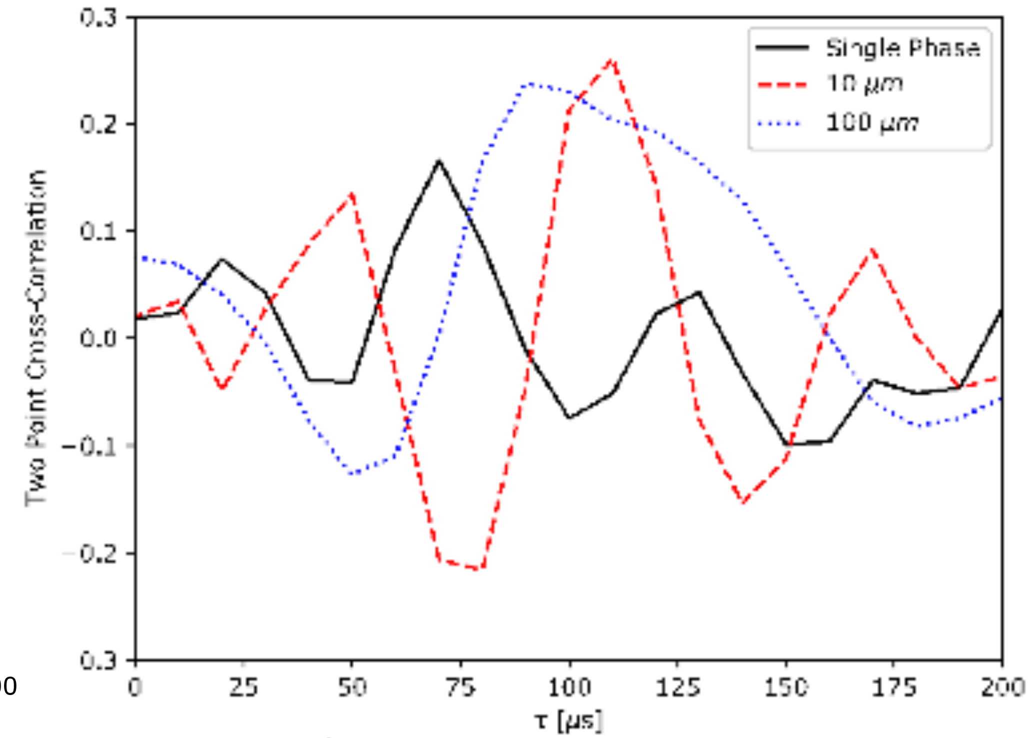

b) $0 \leq \tau \leq 200 \mu s$

$X_1 = D_e, X_2 = 2D_e, Y_1 = Y_2 = D_e.$

Jet condition: $M_j = 1.5, TTR = 1.1, NPR = 3.67.$

Cross-Correlation of Lighthill's Stress Tensor with Various Streamwise Separation, r

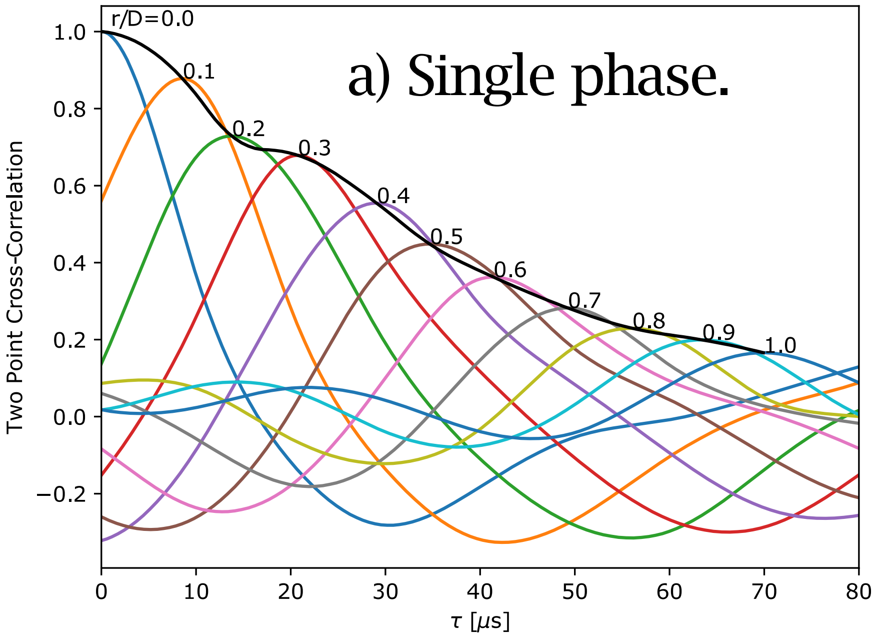

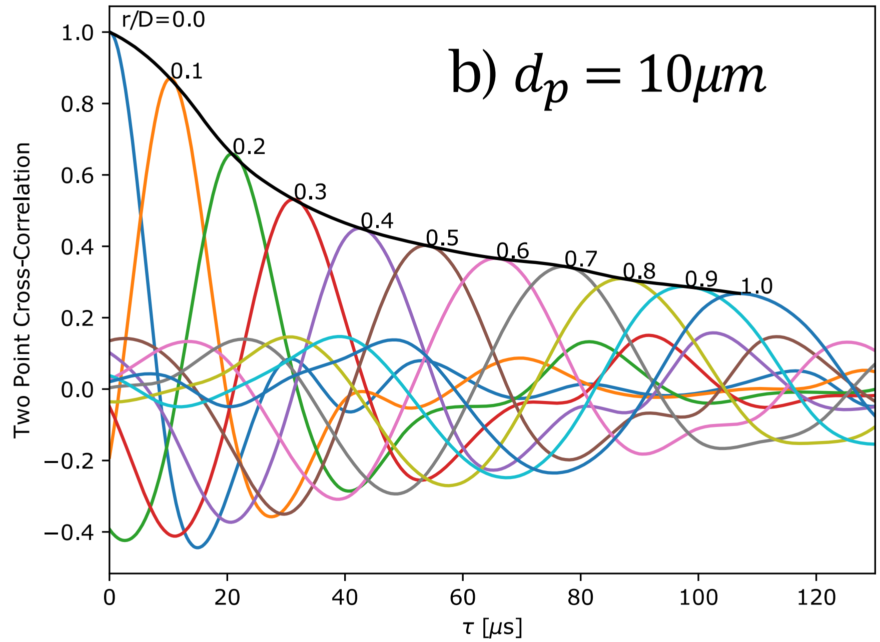

$X_1 = D_e, Y_1 = D_e,$

$\frac{r}{D} = 0, 0.1, 0.2, \ldots, 1.0.$

Jet condition:

$M_j = 1.5, TTR = 1.1,$

$NPR = 3.67.$

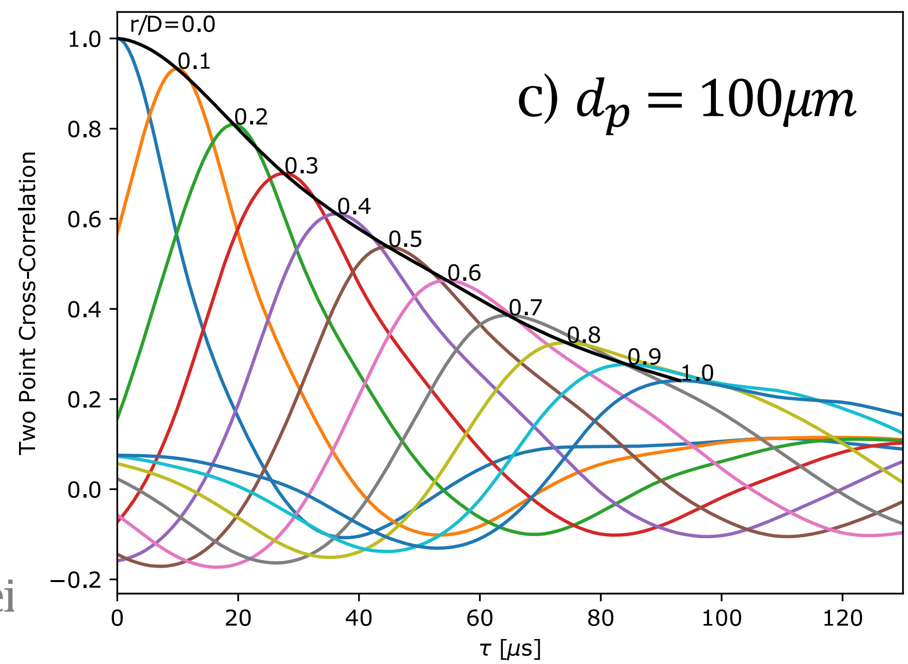

Comparison of SPL Spectra with Various Particle Diameters

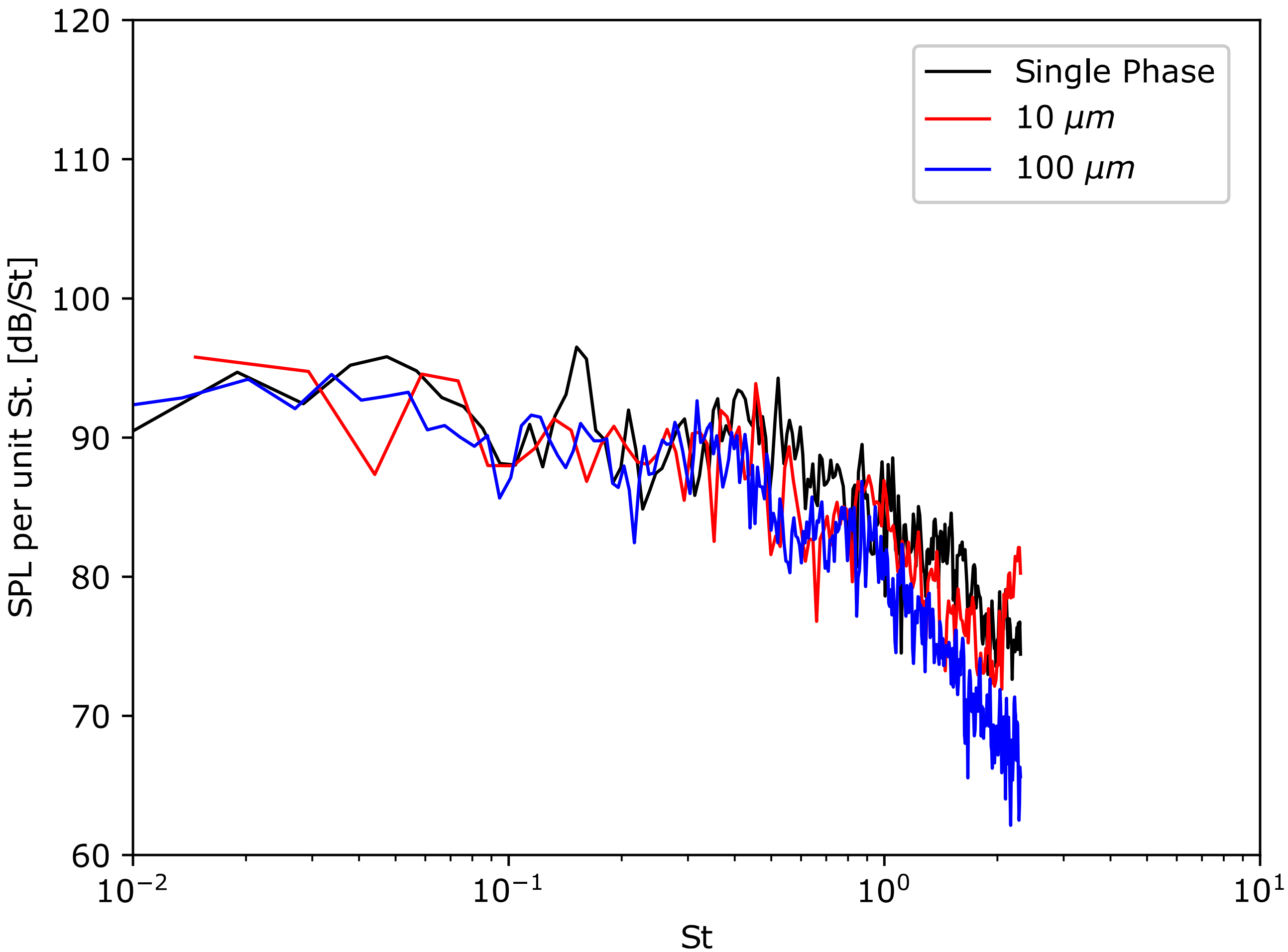

$$\theta = 90^{\circ}, \frac{R}{D_e} = 40, M_j = 1.5, TTR = 1.1$$

- Sideline
- Fine-scale mixing noise
- Plate interference
- Attenuation at high frequency

Comparison of SPL Spectra with Various Particle Diameters

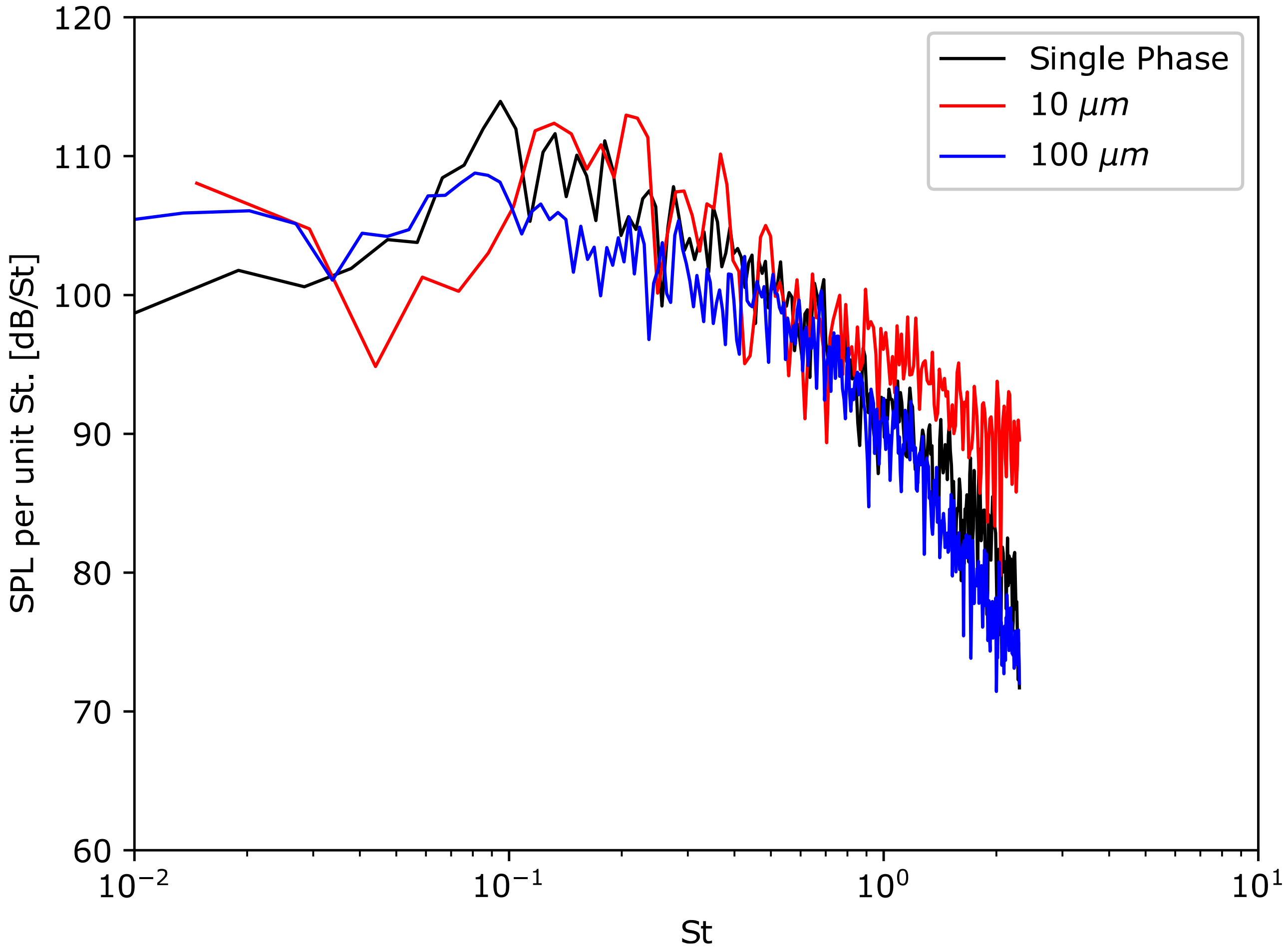

$$\theta = 152^{\circ}, \frac{R}{D_e} = 40, M_j = 1.5, TTR = 1.1$$

- Downstream
- Large-scale mixing noise
- Mach wave radiation
- Attenuation and amplification at high frequency

Summary and Conclusion

Summary and Conclusion

- Summary
  - FWH method based on implicit LES two-phase gas-particle simulation
  - Predictions agree with previous experiments

- Important findings
  - 10 μm particles have low impact on the flow statistics
  - Jet flow with 100 μm particles shows lower mean velocity
  - Particles attenuate high frequency noise at sideline direction
  - Different size of particles shows different impact on the noise downstream

Future Work

- Three-dimensional simulation of two-phase gas-particle supersonic jet flow to capture three-dimensional turbulent break down
- Study the heated jet condition
- Validate with related experimental data
- Apply acoustic analogies to obtain better understanding of sound source

Thank You